



HAL
open science

Intracerebral correlates of scalp EEG ictal discharges based on simultaneous stereo-EEG recordings

Mickaël Ferrand, Cédric Baumann, Olivier Aron, Jean-Pierre Vignal, Jacques Jonas, Louise Tyvaert, Sophie Colnat-Coulbois, Laurent Koessler, Louis Maillard

► To cite this version:

Mickaël Ferrand, Cédric Baumann, Olivier Aron, Jean-Pierre Vignal, Jacques Jonas, et al.. Intracerebral correlates of scalp EEG ictal discharges based on simultaneous stereo-EEG recordings. *Neurology*, 2023, 100 (20), pp.e2045-e2059. <10.1212/WNL.000000000207135>. <hal-04058926>

HAL Id: hal-04058926

<https://hal.science/hal-04058926v1>

Submitted on 5 Apr 2023

HAL is a multi-disciplinary open access archive for the deposit and dissemination of scientific research documents, whether they are published or not. The documents may come from teaching and research institutions in France or abroad, or from public or private research centers.

L'archive ouverte pluridisciplinaire **HAL**, est destinée au dépôt et à la diffusion de documents scientifiques de niveau recherche, publiés ou non, émanant des établissements d'enseignement et de recherche français ou étrangers, des laboratoires publics ou privés.



Distributed under a Creative Commons CC BY-NC 4.0 - Attribution - Non-commercial use - International License

Intra-cerebral correlates of scalp EEG ictal discharges

based on simultaneous recordings

Mickaël FERRAND, Cédric BAUMANN, Olivier ARON, Louise TYVAERT, Sophie COLNAT-COULBOIS, Jean-Pierre VIGNAL, Laurent KOESSLER, and Louis MAILLARD

SUMMARY

Background and Objectives: It remains unknown to what extent ictal scalp EEG can accurately predict the localization of the intra-cerebral seizure onset in pre-surgical evaluation of drug resistant epilepsies. In this study, we aimed to define homogeneous ictal scalp EEG profiles (based on their first ictal abnormality) and assess their localizing value using simultaneously recorded scalp EEG and Stereo-EEG.

Methods: We retrospectively included consecutive patients with drug-resistant focal epilepsy who had simultaneous stereo-EEG and scalp EEG recordings of at least one seizure, in the epileptology unit in Nancy, France. We analyzed one seizure per patient and used hierarchical cluster analysis to group similar seizure profiles on scalp EEG and then performed a descriptive analysis of their intra-cerebral correlates.

Results: We enrolled 129 patients in this study. The hierarchical cluster analysis showed six profiles on scalp EEG first modification. None was specific to a single intra-cerebral localization. The “normal EEG” and “blurred EEG” clusters (early muscle artifacts) comprised only five patients each and corresponded to no preferential intra-cerebral localization. The “temporal discharge” cluster (n=46) was characterized by theta or delta discharges on ipsilateral anterior temporal scalp electrodes and corresponded to a preferential mesial temporal intra-cerebral localization. The “posterior discharge” cluster (n=42) was characterized by posterior ipsilateral or contralateral rhythmic alpha discharges or slow waves on scalp and corresponded to a preferential temporal localization. However, this profile was the statistically most frequent scalp EEG correlate of occipital and parietal seizures. The “diffuse suppression” cluster (n=9) was characterized by a bilateral and diffuse background activity suppression on scalp and corresponded to mesial, and particularly insulo-opercular, localization. Finally, the “frontal discharge” cluster (n=22) was characterized by bilateral frontal rhythmic fast activity or pre-ictal spike on scalp and corresponded to preferential ventrodorsal frontal intra-cerebral localizations.

Discussion: Hierarchical cluster analysis identified six seizure profiles regarding the first abnormality on scalp EEG. None of them was specific of a single intra-cerebral localization. Nevertheless, the strong relationships between the “temporal”, “frontal”, “diffuse suppression” and “posterior” profiles and intra-cerebral discharges localizations may contribute to hierarchize hypotheses derived from ictal scalp EEG analysis regarding intra-cerebral seizure onset.

KEYWORDS: Stereo-electroencephalography, drug resistant epilepsy, focal epileptic seizures, simultaneous recordings, localization, lateralization, epileptogenic zone

INTRODUCTION

Although most of operated drug resistant focal epilepsies are related to a histologically identified lesion, MRI or PET imaging cannot localize alone the epileptogenic zone (EZ)¹⁻⁴. The sensitivity, specificity, and accuracy of combined MRI and PET for seizure onset localization were estimated around 95%, 9%, and 65%, respectively regardless of the etiology and localization³. Therefore, there is now a consensus about the fact that delineating the corticectomy and defining a strategy of intra-cranial or intra-cerebral exploration shall rely on a multimodal approach including long-term video-EEG recordings⁵.

However, It has been established that scalp EEG does not accurately predict the localization and lateralization of the EZ^{6,7}. According to Casale et al., only 58% of the seizures detected on Stereo-EEG (SEEG) are visible on scalp EEG and 33% of focal aware or subclinical seizures⁶. Spencer et al. showed an agreement between scalp EEG and depth electrodes of 21 to 38% for lobe localization and 46 to 49% for lateralization of seizure onset⁷. This is even more evident for certain EZ lobar localization, notably frontal and parietal epilepsies⁸⁻¹¹. In another study, only 40% of the patients with epilepsy who underwent surgery had an EZ localized in the correct lobe before invasive subdural grids

examination¹¹. Therefore, in many cases, intra-cranial or intra-cerebral explorations by electro-corticography or SEEG are necessary to localize and delineate the area to be operated on with precision and map the functional areas^{12,13}. Few studies have validated the results of scalp EEG using SEEG as a gold standard. Even fewer studies combined simultaneous recordings^{14–21} which should be the best approach to show correlations between SEEG and scalp EEG. These studies did not include more than 24 patients. Most of these studies focused only on temporal lobe seizures. For the others, the extra-temporal localizations were limited to the frontal lobe and with a very small number of patients^{15–17,19}. Some automatic electrical signal processing algorithms have been developed and validated to help localize the EZ (source localization)^{17–24}. However, no study has correlated scalp EEG and SEEG localization with simultaneous recordings of epileptic seizures regardless of their intra-cerebral lobar localization.

In this study, we aimed to define homogeneous ictal scalp EEG profiles (based on their first ictal modification) and assess their intra-cerebral correlates using simultaneously recorded scalp EEG and Stereo-EEG.

MATERIALS & METHODS

Patients

We retrospectively included patients who had a simultaneous EEG and SEEG recording between October 2007 and December 2021 in the epilepsy monitoring unit, Neurology department of the Nancy Hospital, France, from a prospective in-hospital database. These 210 patients were extracted from a database of 303 SEEGs, performed in 278 patients. Patients with poor scalp EEG coverage, non-interpretable scalp EEG because of major technical artifacts, no recorded seizure or non-localizing SEEG were then excluded. All patients who underwent SEEG were drug-resistant and had previously completed a non-invasive pre-surgical phase, including video-EEG, brain MRI (with coronal 3D T1 FSPGR high resolution-weighted images, axial T2* weighted images, coronal T2 FSEIR and sagittal 3D FLAIR), FDG PET brain scan, neuropsychology assessment, psychiatric consultation²⁵. All included patients agreed to participate in this study.

Implantation and recording

The electrodes scheme was determined according to the electro-clinical hypotheses derived from non-invasive multi-modal phase 1 findings put together during a multidisciplinary case management conference. Implantation of SEEG electrodes was performed according to the previously described methodology (Salado et al., 2018 and eAppendix 1, for more details)²⁵. Installation of scalp electrodes was performed 24 hours after implantation of intra-cerebral electrodes according to the 10-20 or 10/10 system under sterile conditions and using sterile Ag/AgCl electrodes (cf eAppendix 1 for a detailed description).

Interpretation and constitution of the database

For each included patient, we selected the most representative usual seizure, with the best possible quality, to avoid overrepresentation of patients with multiple seizures. Scalp EEG recordings were analyzed by an experienced epileptologist (MF) blinded to the SEEG recordings but familiar with the history of the patients as well as the results of their imaging explorations, to determine the onset, morphology, and localization of the ictal discharges. All intra-cerebral recordings were reviewed during the multidisciplinary post-SEEG case management conference, allowing to draw consensual conclusions regarding the epileptogenic zone localization and functionality and archived in the in-hospital database. These conclusions, as well as the characteristics of the intra-cerebral discharges were extracted, double-checked, and classified by an experienced epileptologist (MF) for the purpose of the study. The data were then cross tabulated to determine the time delay between the changes in SEEG and the scalp EEG. A second reading of the scalp EEG was performed by another epileptologist (LM) on 33 randomly selected seizures to perform a Cohen's kappa.

The morphology of the first ictal abnormality on scalp EEG was classified as follows: "artifact" (when EEG was blurred by muscle artifacts), "low voltage fast activity" (LVFA) if frequency ≥ 30 Hz and amplitude < 25 uV, "rhythmic fast activity" (RFA) if ≥ 13 Hz and < 30 Hz, "rhythmic slow activity" (RSA) if < 13 Hz (with a subdivision into alpha (8 to 12Hz), theta (4 to 7Hz) and delta (< 4 Hz) discharge), "suppression" if amplitude < 10 uV²⁸, "periodic activity", "sharp wave", "slow wave". Lateralization was collected as ipsilateral, contralateral to the EZ in SEEG, or bilateral. The scalp EEG localization was categorized as follows: Fz, Cz, Pz, Oz, Fp2F4-Fp1F3, F4C4-F3C3, P4-P3, O2-O1, F8T8Ft10-F7T7Ft9, P8P10-P7P9. The seizure duration, delay between the SEEG and scalp EEG onset were collected. If no abnormalities

were visible on the scalp EEG, it was qualified as normal and the morphological characteristics were noted as not available.

The morphology of the first intra-cerebral ictal discharge on SEEG was classified according to the same terminology: "suppression", "LVFA", "RFA", "RSA". The SEEG localization of the intra-cerebral ictal discharge (presumed EZ) was categorized in several sub-lobar, lobar or multilobar regions of interest: prefrontal (PF), premotor or motor (PM/M), extended frontal (PF + PM/M), insulo-opercular, temporal, occipital, parietal, parieto-occipital, fronto-parietal, temporo-parietal, temporo-occipital or fronto-parieto-occipital. We also collected the depth of the EZ, i.e. mesial, lateral, or mesio-lateral. As well as the ventro-dorsal gradient, i.e. dorsal, ventral or ventro-dorsal. Lateralization and duration of the seizure were also collected.

Statistical analyses

Description of data

Continuous variables (all following a normal distribution) were characterized by their mean and standard deviation and qualitative variables by their number and percentage. Comparisons of means were performed using a Student's t-test and comparisons of proportions using a Chi² test or Fisher's exact test if necessary.

Interobserver agreement on scalp EEG data

First step was to validate the interpretation of the scalp EEGs by applying a Cohen's Kappa test between the interpretation of the two epileptologists on a quarter of the included seizures (33/129). The percentage of agreement was achieved on several points: morphology of the initial ictal abnormality (as described previously), main localization on scalp electrodes, and laterality. The localization was grouped in one variable with several modalities, i.e. frontal (Fp2, Fp1, F4, F3, C4, C3, Fz, Cz), temporal (F8, F7, T8, T7, P8, P7, Ft10, Ft9, P10, P9), parieto-occipital (P4, P3, O2, O1, Pz, Oz), combinations of frontal and temporal, frontal and parieto-occipital, temporal and parieto-occipital, hemispheric, or without abnormality. We used Landis and Koch's 1977 classification to characterize the strength of agreement: disagreement if less than or equal to 0, a weak agreement between 0 and 0.20, a confident agreement between 0.21 and 0.40, a moderate agreement between 0.41 and 0.60, a substantial agreement between 0.61 and 0.80, and almost perfect agreement between 0.81 and 1. In cases of discrepancies, a collegial review allowed to reach a consensual interpretation.

Characterization of scalp EEG profiles

After validating our interpretation of the scalp EEGs on the simplified variables described above, we used the complete data mentioned in the paragraph "interpretation and constitution of the database" to perform the analysis. A hierarchical cluster analysis was performed to group patients with similar seizures in terms of their variables regarding morphology and localization of scalp EEG first abnormality. The inertia gain graph allowed us to decide how many classes to perform with a decision to stop when the inertia gain reaches a plateau i.e., when the addition of an extra group does not explain more of the variability between individuals than the group before. For better readability, only the modalities of the variables that significantly characterized each class were described. That is, the variables that were significantly more frequent in one cluster than in the other clusters taken together. Significance was defined as a p-value <0.05. We performed statistical analyses using R software (version 4.1.1; R Core Development Team 2021) and the FactoShiny package. This analysis was performed on scalp EEG data alone to allow differentiation of profiles that epileptologists may encounter in clinical practice who do not have access to SEEG data.

Description of SEEG data for each of the selected profiles

Once the different profiles were delineated, the characteristics of the intra-cerebral discharges on SEEG corresponding to each cluster were described according to the previously stated variables, with their median and inter-quartile range (IQR) for quantitative data (not following the normal distribution for all of them), with their number and percentage for qualitative data. We performed statistical tests to compare the SEEG data of each cluster with the others via Chi-square, and Fisher tests according to the respective application conditions.

Standard Protocol Approvals, Registrations, and Patient Consents

All patients signed a generic information and consent form for the use of their personal clinical data according to the French law, validated by the institutional ethics board of the Nancy university Hospital, and were informed by letter of this retrospective study, and of the possibility of objecting to their participation.

RESULTS

General characteristics

Of the 210 patients who underwent simultaneous EEG and SEEG recordings, we included 129 patients who met the inclusion criteria. Patients with poor scalp coverage, non-interpretable scalp EEG, without seizure recorded or with non-localizing SEEG were excluded from the analysis (Figure 1). Among these 129 included patients, 58.9% were men, the average age was 12.5 (SD = 9.7) years at epilepsy onset and 30.1 (SD = 10.3) years at the time of the SEEG, with a delay of 17.7 (SD = 10.7) years. The most frequent etiologies were focal cortical dysplasia type 1 or 2 (25.6%), hippocampal sclerosis (20.9%), and dysembryoplastic neuroepithelial tumor (DNET) or ganglioglioma (10.9%). The cause was unknown in 24.8% of patients. Brain MRI and FDG PET scans performed during the evaluation were normal in 35.7% and 14.4% of cases, fully concordant with the SEEG localization of the EZ in 22.5% and 21.6%, not concordant in 3.1% and 7.2%, partially concordant in 38.8% and 56.8% respectively. The average number of SEEG electrodes implanted was 13.2 per patient. The average number of surface EEG electrodes was 24.7 per patient. A majority of analyzed seizures were left-sided (56.6%). The EZ included the frontal lobe in 27.9% of the patients, the temporal lobe in 55.8%, the parietal lobe in 16.3%, the occipital lobe in 6.2%, and the insular lobe in 21.7%. A corticectomy was performed in 70.5% of the patients with an average postsurgical follow-up of 2.9 years. The anatomopathological analysis found in the majority a focal cortical dysplasia type 2 (25.3%), hippocampal sclerosis (24.2%), a DNET, or a ganglioglioma (13.2%). The Engel score at the last follow-up was classified as IA in 60.4% of patients. Included and excluded patients were comparable for all these variables except for sex, percentage of operated patients, and the side of the EZ due to the presence of bilateral epilepsies in excluded patients (for more details, see Table 1).

Interobserver agreement on scalp EEG data

The interobserver agreement for the first abnormality was almost perfect for morphology (0.95), substantial for laterality (0.78) and for localization (0.73).

Characterization of scalp EEG profiles on the 1st abnormality and description of SEEG data

The hierarchical cluster analysis of the first abnormality in scalp EEG of the 129 analyzed seizures identified 6 groups with a similar EEG profile. The inertia gain graph allowed us to determine the number of clusters retained with a decision to stop when the inertia gain reaches a plateau i.e., when the addition of an extra group does not explain more of the variability between individuals than the previous group (Figure 2). The description of the different clusters and the analysis of the linked SEEG data are presented in Table 2.

The first cluster (n=5), going from left to right on the dendrogram, was constituted of EEG without abnormality ($p < 0.001$) and coined "normal EEG".

The second cluster (n=5) was characterized by early muscle artifacts ($p < 0.001$) and coined "blurred EEG".

The third cluster (n=46) was characterized by slow theta ($p < 0.001$) or delta ($p < 0.001$) rhythmic activities on the F8T8Ft10-F7T7Ft9 electrodes ($p < 0.001$), ipsilateral to the intra-cerebral seizure onset ($p < 0.001$) and coined "temporal discharge". The scalp EEG ictal discharges lasted mostly between 30 and 60 seconds ($p = 0.047$).

The fourth cluster (n=42) was characterized by more frequent ipsilateral ($p = 0.006$) or contralateral ($p = 0.033$) alpha rhythmic activity ($p < 0.001$) or slow waves ($p < 0.001$) at the P4-P3 ($p < 0.001$), O2-O1 ($p < 0.001$), or P8P10-P7P9 ($p = 0.012$) electrodes. It was coined "posterior discharge". In this cluster, 2 out of 3 patients with a contralateral scalp EEG discharge had bilateral implantation. The last one had a unilateral implantation, guided by lateralizing ictal sign and MRI structural abnormality and had a favorable post-surgical seizure outcome (Engel Ia). Interestingly these 3 patients were the only patients of the whole cohort with strictly contralateral EEG initial discharge. Two patients had bilateral posterior EEG discharge: one had a bilateral implantation. In the other, unilateral implantation was guided by lateralizing ictal sign and MRI abnormality

The fifth cluster (n=9) was characterized by a diffuse and bilateral (p=0.008) suppression of the background activity (p<0.001), on all the scalp electrodes (p-values from <0.001 to 0.042 depending on the localization). It was coined “diffuse suppression”.

The last cluster (n=22) was characterized by more frequent bilateral (p<0.001), rhythmic fast activity (p<0.001) or preictal spike on Fp2F4-Fp1F3 (p<0.001), F4C4-F3C3 (p<0.001), Fz (p<0.001), Cz (p<0.001) electrodes. Regarding patients with bilateral frontal discharge (n=12), 10 had contralateral sentinel electrodes (n= 1 to 5). The two remaining patients had a unilateral implantation guided either by clinical (n=1) or MRI (n=1) lateralizing sign and had both a favorable seizure outcome (Engel Ia). This profile was coined “frontal discharge”.

The “normal EEG” profile corresponded to short (median=21.0 sec, IQR=4.0-28.0) intracerebral seizures, with high frequency discharges (median=38.0Hz, IQR=22.0-50.0). There was no preferential localization at seizure onset (2 prefrontal, 1 extended frontal, 1 temporal, 1 insulo-opercular).

The “blurred EEG” profile corresponded to rather prolonged intra-cerebral seizures (median=76.0 sec, IQR=24.0-87.0), with high frequency discharges (median=29.0Hz, IQR=17.0-68.0). There was no preferential localization at seizure onset (1 prefrontal, 1 extended frontal, 2 temporal, and 1 insulo-opercular).

The “temporal discharge” profile corresponded to prolonged intra-cerebral seizures (median=86.5 sec, IQR= 56.8-127.8), characterized by slow rhythmic (19/46), or fast low voltage discharges (18/46) with a median frequency of 17.5, IQR=6.5-48.0. The localization at seizure onset was mainly temporal (37/47) and this localization was statistically more frequent in this cluster (p<0.001). The localization at seizure onset could however also be prefrontal (n=3), premotor or motor (n=1), extended frontal (n=2), parietal (n=2), and insulo-opercular (n=1). Mesial (32/46, p=0.011) and ventral (34/46, p<0.001) onsets were statistically more frequent in this profile.

The “posterior discharge” profile corresponded to intermediate duration (median=64.5 sec, IQR=27.5-97.3), intra-cerebral seizures characterized by high frequency discharges (median=46.0Hz, IQR=13.0-80.0). The localization at seizure onset was mainly temporal (18/42) but a parietal onset (7/42) as well as an occipital onset (3/42) were statistically more frequent in this profile (7 of the 10 parietal onset seizures in the whole cohort, p=0.014; 3 out of the 3 occipital onset seizures in the whole cohort, p=0.033). Other localizations at seizure onset could be insulo-opercular (4/42), prefrontal (2/42), and multilobar (8/42). An example of a simultaneous recording of a left parieto-occipital sulcus seizure with a posterior discharge on scalp EEG is presented in Figure 3B.

The “diffuse suppression” profile corresponded to prolonged duration (median=75.0 sec, IQR=45.0-93.0) intra-cerebral seizures characterized by high frequency discharges (median= 40.0Hz, IQR=24.0-45.0). The localization at seizure onset was mainly temporal (5/9) but an insulo-opercular onset was statistically more frequent in this cluster than in the other (3/9, p=0.047). Other localization at seizure onset could be premotor or motor (1/9). Most intra-cerebral seizures had a mesial (6/9) and/or ventral (5/9) onset.

The “frontal discharge” profile corresponded to intermediate duration (median=45.0 sec, IQR=14.3-107.8) intracerebral seizures characterized by high frequency discharges (median=33.0Hz, IQR=14.3-72.5). The localizations at seizure onset were mainly frontal (12/22 distributed in 3 prefrontal; 4 premotor or motor; 5 extended frontal) and these localizations were statistically more frequent in this profile (p=0.008 for premotor or motor onset, p=0.007 for extended frontal onset). Additional localizations at seizure onset could be temporal (4/22), fronto-parietal (2/22), and parietal (1/22). The seizures were rather ventrodorsal (10/22, p=0.003). An example of a simultaneous recording of a right motor cingulate onset seizure with rapid propagation to the left motor cingulate and supplementary motor area is presented in Figure 3A. Figure 4 summarizes the correlations between scalp EEG discharge and intracerebral seizure onset localizations.

Duration of the intra-cerebral discharge was significantly different between the different profiles (Kruskall Wallis test, p=0.006). The longest average intra-cerebral discharges was associated with the “temporal discharge” cluster while the shortest was associated with the “normal EEG” cluster (cf table 2).

DISCUSSION

First, our cohort is comparable to a previous multicenter SEEG study, in terms of seizure outcome with a 60.4% and 82.4% Engel Ia and Engel I respectively, and a mean follow-up of 3 years²⁹.

In this study, we aimed to define homogeneous ictal scalp EEG profiles (based on their first ictal abnormality) using hierarchical cluster analysis and assess their localizing value using simultaneously recorded scalp EEG and Stereo-EEG. This methodology allowed identifying 6 clusters regarding ictal scalp EEG first modification: the “normal EEG”, “blurred EEG”, “temporal discharge”, “posterior discharge”, “diffuse suppression” and “frontal discharge” profiles.

The “normal EEG” and “blurred EEG” profiles represented few patients and were not localizing. The “temporal discharge” profile was well lateralizing and included 81% of seizures of temporal origin, 70% of mesial and 74% of ventral discharges. The “posterior discharge” profile was not lateralizing and included 43% of seizures of temporal origin. However, all occipital seizures and 70% of parietal seizures in the sample were in this cluster. The “diffuse suppression” profile included 67% of mesial seizures, 56% of temporal origin, and 33% of insulo-opercular origin, the latter being statistically more represented in this group than in the others. The “frontal discharge” profile was not lateralizing and included 64% of seizures of frontal origin (55% unilobar, 9% multilobar). The seizures were often dorsoventral.

First, we can note the absence of specific intracerebral localization for any of the surface profiles. Indeed, the scalp EEG can be inaccurate due to the presence of artifacts, the biophysical attenuation of the EEG signal by the brain, bone, and scalp compartments, the distance between the sources of the signal and the scalp electrodes (especially if the origin of the seizures is located on the mesial face of the brain or in the depth of a sulcus). The orientation of the intra-cerebral electrical fields according to the geometric configuration of the cortex, the mix of several simultaneous sources, the connectivity of the epileptic sources and the more or less rapid propagation of the ictal discharges can also make the scalp EEG less efficient³⁰⁻³². Finally, from a theoretical point of view, the multiple solutions to the inverse problem, i.e. the multiple intra-cerebral solutions for a single localization in scalp EEG, makes topographical inferences from scalp EEG uncertain²². This first conclusion is essential for the clinician who should not rely solely on the interpretation of the scalp EEG to make his assumptions about the localization of the epileptogenic zone. This interpretation should always be done in association with the ictal clinical signs, as well as the imaging data, and the neuropsychological assessment.

Secondly, our “*inverse problem*” approach consisted in starting from the description of scalp EEG patterns and then assess its intra-cerebral localizing value, i.e. describing the related intra-cerebral possible seizure onsets. This methodology is very original when considering previous EEG-SEEG correlation studies. This choice was made on purpose to follow the timeline and the logic of the clinician's reasoning, who must establish hypotheses at the end of the first phase of the pre-surgical assessment, to guide direct surgery or SEEG implantation strategy. This methodology allowed us to identify 6 profiles, of which 3 stood out by their size, the temporal, posterior and frontal discharges profiles.

The clearest described profile in the literature is the “temporal discharge” profile with an ipsilateral anterior temporal rhythmic theta or delta discharge on the scalp EEG³³. This surface pattern corresponded significantly to mesial temporal seizures in SEEG. But even in this group, 20% of the seizures had an extratemporal onset. We found 13% of seizures of frontal origin, which can be explained by the privileged propagation of these seizures to the temporal lobe via the arcuate and uncinata fascicles or by the biophysical projection of certain prefrontal generators, especially the orbito-frontal, on the anterior temporal scalp electrodes³⁴. The remaining 7% are parietal and insulo-opercular seizures. Parietal seizures may rapidly propagate to the temporal lobe via inferior division of the superior longitudinal fascicle, the middle longitudinal fascicle and the arcuate fascicle³⁵, insular seizures to the temporal operculum through short distances connections.

The “Posterior discharge” cluster presenting as posterior alpha discharges or slow waves on scalp EEG were neither lateralizing nor perfectly localizing. The absence of lateralization is explained by the great trans-callosal connection of the occipital lobes³⁶. This bilateral aspect in scalp EEG has already been described previously¹¹. The presence of 43% of seizures of temporal origin in this cluster can be explained by the posterior temporal seizures, which can be projected on the posterior temporal or even parieto-occipital scalp electrodes, but also, by the white matter pathways linking the temporal lobe to the parietal and occipital lobes, i.e. the arcuate fascicle, the third branch of the superior

longitudinal fascicle, the middle longitudinal fascicle, the ventral visual pathway via the inferior longitudinal fascicle^{35,36}. The few seizures of prefrontal origin visible on the posterior scalp electrodes can be explained by propagation via the superior and middle divisions of the superior longitudinal fascicle³⁴ and the insulo-opercular seizures spread via the parietal operculum.

The "frontal discharge" profile was non-lateralizing and had a moderate localizing value. The bilateral visibility in scalp EEG is explained by the rapid passage of discharges through the corpus callosum and the anterior white commissure³⁴. The presence of seizures of extra-frontal origin (18% of temporal, 5% of parietal and 14% of insulo-opercular origin) projecting to the frontal scalp electrodes is explained by the connection of all the other lobes to the frontal lobe via the arcuate, uncinata, superior, middle, and inferior longitudinal fascicles, as well as the inferior fronto-occipital fascicle³⁴.

Finally, the "diffuse suppression" cluster was small but could orient towards mesial temporal or insulo-opercular onset (this last one being more frequent in this cluster than in others) and could be a good temporal marker of intra-cerebral seizure onset with a median delay of 1 second.

Limitations and strengths

The originality and strength of our study is the use of a hierarchical cluster analysis to describe the scalp EEG ictal profiles and the use of simultaneous SEEG-EEG recordings to describe their intra-cerebral correlates. We selected this methodology because of the unsupervised nature of this analysis, i.e. the realization of classification without any preconceived ideas about the included variables. The clustering was performed on scalp EEG data alone to respect the timeline of clinical reasoning during pre-surgical investigations. The last strength of our study is the presence in our sample of the totality of the seizure lobar localizations.

Included and excluded patients were similar in all demographic characteristics except for the sex. The included patients were predominantly male. We found no obvious explanation to this difference, but we believe that this had no effect on our analysis because seizure localization is not known to be correlated with sex. We additionally found a higher percentage of operations in the included group which can be explained by the presence of patients with non-localizing SEEG or no recorded seizures in the excluded group. Finally, the number of patients with a normal scalp EEG is small. This can be explained by the selection of the more informative seizure (with visible abnormality) per patient for analysis in cases of multiple recorded seizures. Therefore, this value does not reflect the real sensitivity of scalp EEG to intracerebral discharges. This normal pattern had no specific localizing value but corresponded to the shortest intra-cerebral seizures.

Finally, simultaneous SEEG-EEG recordings bears the theoretical risk of breach rhythm and volume conduction distortion. The absence of these artifacts in our study can be explained by the small size of the skull's hole (2.45mm-diameter), the low electrical conductivity of the guidance screw (titanium), and the safety distance between the scalp electrode and the entry point. We previously validated the EEG volume conduction in the setup of simultaneous EEG-SEEG across in several studies^{16,27,37,38}.

Perspectives

Future studies, adding relevant clinical variables and data regarding the pattern of propagation of the scalp EEG discharge could improve the prediction of the epileptogenic zone localization derived from video-EEG recordings.

A more precise description of scalp EEG correlates of intra-cerebral seizures (*direct problem*) based on simultaneous EEG and SEEG recordings should also be carried out, as these have been scarcely described and in very few patients.

CONCLUSION

Our study showed that no surface EEG ictal pattern is specific to a single intracerebral localization of the seizure onset. However, the characterization of these patterns should contribute to better hierarchize hypotheses regarding the epileptogenic zone localization derived from ictal scalp EEG, hopefully leading to improve intra-cranial SEEG implantations or direct surgery strategies.

REFERENCES

1. Blumcke I, Spreafico R, Haaker G, et al. Histopathological Findings in Brain Tissue Obtained during Epilepsy Surgery. *N Engl J Med*. 2017;377(17):1648-1656. doi:10.1056/NEJMoa1703784
2. Maillard LG, Tassi L, Bartolomei F, et al. Stereoelectroencephalography and surgical outcome in polymicrogyria-related epilepsy: A multicentric study. *Ann Neurol*. 2017;82(5):781-794. doi:10.1002/ana.25081
3. Guo K, Cui B, Shang K, et al. Assessment of localization accuracy and postsurgical prediction of simultaneous 18F-FDG PET/MRI in refractory epilepsy patients. *Eur Radiol*. 2021;31(9):6974-6982. doi:10.1007/s00330-021-07738-8
4. Buch K, Blumenfeld H, Spencer S, Novotny E, Zubal IG. Evaluating the accuracy of perfusion/metabolism (SPET/PET) ratio in seizure localization. *Eur J Nucl Med Mol Imaging*. 2008;35(3):579-588. doi:10.1007/s00259-007-0550-y
5. Tatum WO, Mani J, Jin K, et al. Minimum standards for inpatient long-term video-EEG monitoring: A clinical practice guideline of the international league against epilepsy and international federation of clinical neurophysiology. *Clin Neurophysiol*. 2022;134:111-128. doi:10.1016/j.clinph.2021.07.016
6. Casale MJ, Marcuse LV, Young JJ, et al. The Sensitivity of Scalp EEG at Detecting Seizures—A Simultaneous Scalp and Stereo EEG Study. *Journal of Clinical Neurophysiology*. 2022;39(1):78-84. doi:10.1097/WNP.0000000000000739
7. Spencer SS, Williamson PD, Bridgers SL, Mattson RH, Cicchetti DV, Spencer DD. Reliability and accuracy of localization by scalp ictal EEG. *Neurology*. 1985;35(11):1567-1575. doi:10.1212/wnl.35.11.1567
8. Akimura T, Fujii M, Ideguchi M, Yoshikawa K, Suzuki M. Ictal onset and spreading of seizures of parietal lobe origin. *Neurol Med Chir (Tokyo)*. 2003;43(11):534-540. doi:10.2176/nmc.43.534
9. Ristić AJ, Alexopoulos AV, So N, Wong C, Najm IM. Parietal lobe epilepsy: the great imitator among focal epilepsies. *Epileptic Disord*. 2012;14(1):22-31. doi:10.1684/epd.2012.0484
10. O'Muircheartaigh J, Richardson MP. Epilepsy and the frontal lobes. *Cortex*. 2012;48(2):144-155. doi:10.1016/j.cortex.2011.11.012
11. Kim CH, Chung CK, Lee SK, Lee YK, Chi JG. Parietal lobe epilepsy: surgical treatment and outcome. *Stereotact Funct Neurosurg*. 2004;82(4):175-185. doi:10.1159/000082206
12. Isnard J, Taussig D, Bartolomei F, et al. French guidelines on stereoelectroencephalography (SEEG). *Neurophysiol Clin*. 2018;48(1):5-13. doi:10.1016/j.neucli.2017.11.005
13. Maillard L, Ramantani G. New recommendations of the IFCN: From scalp EEG to electrical brain imaging. *Clin Neurophysiol*. 2017;128(10):2068-2069. doi:10.1016/j.clinph.2017.07.413
14. Tanaka H, Khoo HM, Dubeau F, Gotman J. Association between scalp and intracerebral electroencephalographic seizure-onset patterns: A study in different lesional pathological substrates. *Epilepsia*. 2018;59(2):420-430. doi:10.1111/epi.13979
15. Pacia SV, Ebersole JS. Intracranial EEG substrates of scalp ictal patterns from temporal lobe foci. *Epilepsia*. 1997;38(6):642-654. doi:10.1111/j.1528-1157.1997.tb01233.x
16. Koessler L, Cecchin T, Colnat-Coulbois S, et al. Catching the invisible: mesial temporal source contribution to simultaneous EEG and SEEG recordings. *Brain Topogr*. 2015;28(1):5-20. doi:10.1007/s10548-014-0417-z
17. Ray A, Tao JX, Hawes-Ebersole SM, Ebersole JS. Localizing value of scalp EEG spikes: a simultaneous scalp and intracranial study. *Clin Neurophysiol*. 2007;118(1):69-79. doi:10.1016/j.clinph.2006.09.010

18. Koessler L, Benar C, Maillard L, et al. Source localization of ictal epileptic activity investigated by high resolution EEG and validated by SEEG. *Neuroimage*. 2010;51(2):642-653. doi:10.1016/j.neuroimage.2010.02.067
19. Merlet I, Gotman J. Reliability of dipole models of epileptic spikes. *Clin Neurophysiol*. 1999;110(6):1013-1028. doi:10.1016/s1388-2457(98)00062-5
20. Cosandier-Rimélé D, Merlet I, Badier JM, Chauvel P, Wendling F. The neuronal sources of EEG: modeling of simultaneous scalp and intracerebral recordings in epilepsy. *Neuroimage*. 2008;42(1):135-146. doi:10.1016/j.neuroimage.2008.04.185
21. Barborica A, Mindruta I, Sheybani L, et al. Extracting seizure onset from surface EEG with independent component analysis: Insights from simultaneous scalp and intracerebral EEG. *Neuroimage Clin*. 2021;32:102838. doi:10.1016/j.nicl.2021.102838
22. Abdallah C, Maillard LG, Rikir E, et al. Localizing value of electrical source imaging: Frontal lobe, malformations of cortical development and negative MRI related epilepsies are the best candidates. *Neuroimage Clin*. 2017;16:319-329. doi:10.1016/j.nicl.2017.08.009
23. Rikir E, Koessler L, Gavaret M, et al. Electrical source imaging in cortical malformation-related epilepsy: a prospective EEG-SEEG concordance study. *Epilepsia*. 2014;55(6):918-932. doi:10.1111/epi.12591
24. Gavaret M, Trébuchon A, Bartolomei F, et al. Source localization of scalp-EEG interictal spikes in posterior cortex epilepsies investigated by HR-EEG and SEEG. *Epilepsia*. 2009;50(2):276-289. doi:10.1111/j.1528-1167.2008.01742.x
25. Salado AL, Koessler L, De Mijolla G, et al. sEEG is a Safe Procedure for a Comprehensive Anatomic Exploration of the Insula: A Retrospective Study of 108 Procedures Representing 254 Transopercular Insular Electrodes. *Oper Neurosurg (Hagerstown)*. 2018;14(1):1-8. doi:10.1093/ons/opx106
26. Seeck M, Koessler L, Bast T, et al. The standardized EEG electrode array of the IFCN. *Clin Neurophysiol*. 2017;128(10):2070-2077. doi:10.1016/j.clinph.2017.06.254
27. Jacques C, Jonas J, Maillard L, Colnat-Coulbois S, Rossion B, Koessler L. Fast periodic visual stimulation to highlight the relationship between human intracerebral recordings and scalp electroencephalography. *Hum Brain Mapp*. 2020;41(9):2373-2388. doi:10.1002/hbm.24952
28. Rikir E, Maillard LG, Abdallah C, et al. Respective Contribution of Ictal and Inter-ictal Electrical Source Imaging to Epileptogenic Zone Localization. *Brain Topogr*. 2020;33(3):384-402. doi:10.1007/s10548-020-00768-3
29. Barba C, Cossu M, Guerrini R, et al. Temporal lobe epilepsy surgery in children and adults: A multicenter study. *Epilepsia*. 2021;62(1):128-142. doi:10.1111/epi.16772
30. Kamali A, Flanders AE, Brody J, Hunter JV, Hasan KM. Tracing superior longitudinal fasciculus connectivity in the human brain using high resolution diffusion tensor tractography. *Brain Struct Funct*. 2014;219(1):269-281. doi:10.1007/s00429-012-0498-y
31. Niedermeyer E. Dipole theory and electroencephalography. *Clin Electroencephalogr*. 1996;27(3):121-131. doi:10.1177/155005949602700305
32. Grech R, Cassar T, Muscat J, et al. Review on solving the inverse problem in EEG source analysis. *J Neuroeng Rehabil*. 2008;5:25. doi:10.1186/1743-0003-5-25
33. Ebersole JS, Pacia SV. Localization of temporal lobe foci by ictal EEG patterns. *Epilepsia*. 1996;37(4):386-399. doi:10.1111/j.1528-1157.1996.tb00577.x
34. Catani M. The anatomy of the human frontal lobe. *Handb Clin Neurol*. 2019;163:95-122. doi:10.1016/B978-0-12-804281-6.00006-9

35. Caspers S, Zilles K. Microarchitecture and connectivity of the parietal lobe. *Handb Clin Neurol*. 2018;151:53-72. doi:10.1016/B978-0-444-63622-5.00003-6
36. Catani M, Jones DK, Donato R, Ffytche DH. Occipito-temporal connections in the human brain. *Brain*. 2003;126(Pt 9):2093-2107. doi:10.1093/brain/awg203
37. Louviot S, Tyvaert L, Maillard LG, Colnat-Coulbois S, Dmochowski J, Koessler L. Transcranial Electrical Stimulation generates electric fields in deep human brain structures. *Brain Stimul*. 2022;15(1):1-12. doi:10.1016/j.brs.2021.11.001
38. Jacques C, Rossion B, Volfart A, et al. The neural basis of rapid unfamiliar face individuation with human intracerebral recordings. *Neuroimage*. 2020;221:117174. doi:10.1016/j.neuroimage.2020.117174

TABLES

	Overall cohort (N = 278)	Included patients (N = 129)	Excluded patients (N = 81)	p-value
Socio-demographic characteristics				
Sex (male)	141 (50.7)	76 (58.9)	33 (40.7)	0.015
Age at epilepsy onset (y)	12.68 (9.59)	12.47 (9.69)	12.75 (9.71)	0.839
Age at SEEG monitoring (y)	29.53 (10.23)	30.14 (10.30)	28.33 (9.95)	0.208
Epilepsy duration at SEEG (y)	16.81 (10.64)	17.66 (10.73)	15.58 (10.87)	0.177
Etiology of the epilepsy				0.850
- FCD (type 1 or 2)	72 (25.9)	33 (25.6)	17 (21.0)	
- Hippocampal sclerosis	61 (21.9)	27 (20.9)	18 (22.2)	
- DNET/Ganglioglioma	26 (9.4)	14 (10.9)	10 (12.3)	
- PMG/Ulegyria/Schizencephaly	12 (4.3)	3 (2.3)	4 (5.0)	
- FCD (type 3)	10 (3.6)	3 (2.3)	4 (5.0)	
- Cavernoma/AVM	7 (2.5)	5 (3.9)	2 (2.5)	
- TSB	4 (1.4)	3 (2.3)	0 (0.0)	
- Post-traumatic	4 (1.4)	3 (2.3)	1 (1.2)	
- Nodular heterotopy	3 (1.1)	2 (1.6)	0 (0.0)	
- Porencephaly	3 (1.1)	2 (1.6)	1 (1.2)	
- Neonatal stroke	2 (0.7)	0 (0.0)	1 (1.2)	
- Pleiomorphic astrocytoma	1 (0.4)	1 (0.8)	0 (0.0)	
- Dysimmune	1 (0.4)	0 (0.0)	0 (0.0)	
- Post-infectious	0 (0.4)	1 (0.8)	0 (0.0)	
- Oligodendroglioma	1 (0.4)	0 (0.0)	0 (0.0)	
- Epidermoid cyst	1 (0.4)	0 (0.0)	0 (0.0)	
- Neurofibromatosis type 1	1 (0.4)	0 (0.0)	0 (0.0)	
- Unknown	69 (24.7)	32 (24.8)	23 (28.4)	
Brain Imaging				
MRI				0.897
- Normal	96 (34.5)	46 (35.7)	28 (34.6)	
- Total match	59 (21.2)	29 (22.5)	18 (22.2)	
- No match	12 (4.3)	4 (3.1)	1 (1.2)	
- Partial match	111 (40.0)	50 (38.8)	34 (42.0)	
FDG PET	N = 267	N = 125	N = 79	0.868
- Normal	42 (15.7)	18 (14.4)	14 (17.7)	
- Total match	53 (19.9)	27 (21.6)	17 (21.5)	
- No match	22 (8.2)	9 (7.2)	7 (8.9)	
- Partial match	150 (56.2)	71 (56.8)	41 (51.9)	
SEEG monitoring				
Number of SEEG electrodes (per patient)	12.99 (2.37)	13.24 (2.37)	13.04 (2.26)	0.535
Number of scalp EEG electrodes (per patient)	NA	24.69 (1.92)	NA	NA
Laterality of the seizure				0.006
- Right	115 (41.4)	56 (43.4)	30 (37.0)	0.441
- Left	151 (54.3)	73 (56.6)	45 (55.6)	0.997
- Bilateral	12 (4.3)	0 (0.0)	6 (7.4)	0.003
Epileptogenic zone				0.639
- Temporal	175 (62.9)	72 (55.8)	52 (64.2)	
- Frontal	72 (25.9)	36 (27.9)	19 (23.5)	
- Insular	56 (20.1)	28 (21.7)	15 (18.5)	
- Parietal	43 (15.5)	21 (16.3)	19 (23.5)	
- Occipital	19 (6.8)	8 (6.2)	7 (8.6)	
Surgery				
Operated patients	184 (66.2)	91 (70.5)	44 (54.3)	0.025
Follow-up after surgery (y)	3.70 (3.04)	2.93 (2.20)	3.61 (3.34)	0.204
Anatomo-pathology	N = 172	N = 91	N = 44	0.310
- Hippocampal sclerosis	41 (23.8)	22 (24.2)	10 (22.7)	
- FCD 1	17 (9.9)	4 (4.4)	5 (11.4)	
- FCD 2	36 (20.9)	23 (25.3)	6 (13.6)	
- FCD 3	20 (11.6)	3 (3.3)	4 (9.1)	
- DNET/Ganglioglioma	19 (11.0)	12 (13.2)	5 (11.4)	
- Gliosis	7 (4.1)	6 (6.6)	8 (18.2)	
- PMG	5 (2.9)	2 (2.2)	0 (0.0)	
- Tuber	3 (1.7)	2 (2.2)	0 (0.0)	
- Ulegyria	2 (1.2)	1 (1.1)	0 (0.0)	
- Cavernoma/AVM	2 (1.2)	2 (2.2)	0 (0.0)	
- Post-traumatic	2 (1.2)	2 (2.2)	0 (0.0)	
- Pleiomorphic astrocytoma	1 (0.6)	1 (1.1)	0 (0.0)	
- Non-contributory	17 (9.9)	11 (12.1)	5 (13.6)	
Engel's class	N = 185	N = 91	N = 44	0.435
- Ia	100 (54.2)	55 (60.4)	26 (59.1)	
- Ib	22 (11.9)	12 (13.2)	3 (6.8)	
- Ic	10 (5.4)	6 (6.6)	1 (2.3)	
- Id	8 (4.3)	2 (2.2)	4 (9.1)	
- II	16 (8.6)	8 (8.8)	4 (9.1)	
- III	11 (5.9)	3 (3.3)	3 (6.8)	
- IV	17 (9.2)	4 (4.4)	3 (6.8)	
- SUDEP	1 (0.5)	1 (1.1)	0 (0.0)	

Table 1: Baseline characteristics of patients

Data are expressed as mean (sd) or number (%)

Statistical analyses were performed between the included and excluded patients.

Abbreviations: AVM = Arteriovenous malformation; DNET = Dysembryoplastic neuroepithelial tumor; FCD = focal cortical dysplasia; MRI = Magnetic resonance imaging; FDG PET = Fluorodesoxyglucose Positron emission tomography; PMG = Polymicrogyria; SEEG = Stereo-electroencephalography; SUDEP = Sudden Unexpected Death in Epilepsy; TSB = Tuberous sclerosis of Bourneville; y = years.

	Cluster 1 violet (N=5) "Normal EEG"	Cluster 2 turquoise (N=5) "Blurred EEG"	Cluster 3 black (N=46) "Temporal discharge"	Cluster 4 green (N=42) "Posterior discharge"	Cluster 5 red (N=9) "Diffuse suppression"	Cluster 6 blue (N=22) "Frontal discharge"	
Hierarchical clustering analysis on scalp EEG	Localization						
	- No abnormality	p<0.001					
	- Fp2F4-Fp1F3				p<0.001	p<0.001	
	- F4C4-F3C3				p<0.001	p<0.001	
	- Fz				p<0.001	p<0.001	
	- Cz				p<0.001	p<0.001	
	- F8T8Ft10-F7T7Ft9			p<0.001	p=0.042		
	- P8P10-P7P9				p=0.012	p=0.004	
	- P4-P3				p<0.001	p<0.001	
	- O2-O1				p<0.001	p<0.001	
	- Pz				p<0.001		
	- Oz				p<0.001		
	Morphology						
			Artifact p<0.001	RSA (delta) p<0.001	RSA (alpha) p<0.001	Suppression p<0.001	RFA p<0.001
				RSA (theta) p<0.001	Slow waves p<0.001		Preictal spike p=0.028
Side							
			Ipsilateral p<0.001	Ipsilateral p=0.006	Bilateral p=0.008	Bilateral p<0.001	
				Contralateral p=0.033			
Duration							
			30-60s p=0.047				
Descriptive analysis of SEEG data for each cluster	Seizure duration (s)*	21.0 (4.0-28.0)	76.0 (24.0-87.0)	86.5 (56.8-127.8)	64.5 (27.5-97.3)	75.0 (45.0-93.0)	45.0 (14.3-107.8)
	Frequency (Hz)#	38.0 (22.0-50.0)	29.0 (17.0-68.0)	17.5 (6.5-48.0)	46.0 (13.0-80.0)	40.0 (24.0-45.0)	33.0 (14.3-72.5)
	Delay between SEEG & scalp EEG onset (s)#	NA	9.0 (5.0-11.0)	2.5 (0.3-13.8)	1.0 (0.0-7.8)	1.0 (0.0-8.0)	0.0 (0.0-5.0)
	Morphology						
	- LVFA	3 (60.0) p=0.667	2 (40.0) p=1	18 (39.1) p=0.231	20 (47.6) p=1	6 (66.7) p=0.306	12 (54.5) p=0.607
	- RFA	2 (40.0) p=0.618	3 (60.0) p=0.132	9 (19.6) p=0.171	13 (31.0) p=0.744	3 (33.3) p=0.709	6 (27.3) p=1
	- RSA	0 (0.0) p=0.332	0 (0.0) p=0.332	19 (41.3) p=0.003	9 (21.4) p=0.689	0 (0.0) p=0.111	4 (18.2) p=0.590
	Localization						
	- Prefrontal	2 (40.0) p=0.058	1 (20.0) p=0.364	3 (6.5) p=0.745	2 (4.8) p=0.502	0 (0.0) p=1	3 (13.6) p=0.398
	- Premotor or motor	0 (0.0) p=1	0 (0.0) p=1	1 (2.2) p=0.420	0 (0.0) p=0.176	1 (11.1) p=0.358	4 (18.2) p=0.008
	- Insulo-opercular	1 (20) p=0.417	1 (20.0) p=0.417	1 (2.2) p=0.032	4 (9.5) p=1	3 (33.3) p=0.047	3 (13.6) p=0.464
	- Temporal	1 (20) p=0.194	2 (40.0) p=0.671	37 (80.4) p<0.001	18 (42.9) p=0.212	5 (55.6) p=1	4 (18.2) p=0.001
	- Occipital	0 (0.0) p=1	0 (0.0) p=1	0 (0.0) p=0.552	3 (7.1) p=0.033	0 (0.0) p=1	0 (0.0) p=1
	- Parietal	0 (0.0) p=1	0 (0.0) p=1	2 (4.3) p=0.493	7 (16.7) p=0.014	0 (0.0) p=1	1 (4.5) p=1
	- Frontal (PF + PM/M)	1 (20) p=0.308	1 (20.0) p=0.308	2 (4.3) p=0.489	0 (0.0) p=0.030	0 (0.0) p=1	5 (22.7) p=0.007
	- Parieto-occipital	0 (0.0) p=1	0 (0.0) p=1	0 (0.0) p=0.537	2 (4.8) p=0.104	0 (0.0) p=1	0 (0.0) p=1
	- Fronto-parietal	0 (0.0) p=1	0 (0.0) p=1	0 (0.0) p=0.552	1 (2.4) p=1	0 (0.0) p=1	2 (9.1) p=0.075
	- Temporo-parietal	0 (0.0) p=1	0 (0.0) p=1	0 (0.0) p=0.537	2 (4.8) p=0.104	0 (0.0) p=1	0 (0.0) p=1
	- Temporo-occipital	0 (0.0) p=1	0 (0.0) p=1	0 (0.0) p=0.537	2 (4.8) p=0.104	0 (0.0) p=1	0 (0.0) p=1
	- Fronto-parieto-occipital	0 (0.0) p=1	0 (0.0) p=1	0 (0.0) p=1	1 (2.4) p=0.326	0 (0.0) p=1	0 (0.0) p=1
	Gradient						
	- Ventral	1 (20.0) p=0.201	2 (40.0) p=0.675	34 (73.9) p<0.001	21 (50.0) p=1	5 (55.6) p=1	3 (13.6) p<0.001
- Dorsal	4 (80.0) p=0.024	1 (20.0) p=1	7 (15.2) p=0.021	14 (33.3) p=0.546	2 (22.2) p=1	9 (40.9) p=0.257	
- Ventro-dorsal	0 (0.0) p=0.582	2 (40.0) p=0.264	5 (10.9) p=0.084	7 (16.7) p=0.651	2 (22.2) p=1	10 (45.5) p=0.003	
Depth							
- Mesial	1 (20.0) p=0.183	2 (40.0) p=0.663	32 (69.6) p=0.011	19 (45.2) p=0.264	6 (66.7) p=0.502	9 (40.9) p=0.287	
- Lateral	2 (40.0) p=0.264	0 (0.0) p=0.582	6 (13.0) p=0.204	12 (28.6) p=0.155	2 (22.2) p=1	4 (18.2) p=1	
- Mesio-lateral	2 (40.0) 0.607	3 (60.0) p=0.114	8 (17.4) p=0.130	11 (26.2) p=1	1 (11.1) p=0.444	9 (40.9) p=0.151	

Table 2: Classification on variables concerning the first scalp EEG abnormality and descriptive analysis of SEEG data for each cluster

Data are expressed as median (IQR) or number (% of total number of seizures in each group) and p-value.

Abbreviations: Hz = Hertz; LVFA = Low-voltage fast activity; M = Motor; PF = Prefrontal; PM = Premotor; RFA = Rhythmic fast activity; RSA = Rhythmic slow activity; s = seconds.

The upper part of the table represents the data from the cluster analysis of the scalp EEG and only statistically significant values are expressed.

The lower part represents the data from the descriptive analysis of the SEEG variables by cluster. The percentage is expressed in relation to the total number in each cluster and the p-values were performed by comparing the modalities of each class to the other classes combined.

* Overall significant difference between clusters (using a Kruskal-Wallis test) with p=0.006. Significant differences are found between clusters 3 and 6, 1 and 3, 1 and 5, 1 and 4 (using a Dunn test).

No significant overall difference between clusters (using a Kruskal-Wallis test).

FIGURES AND LEGENDS

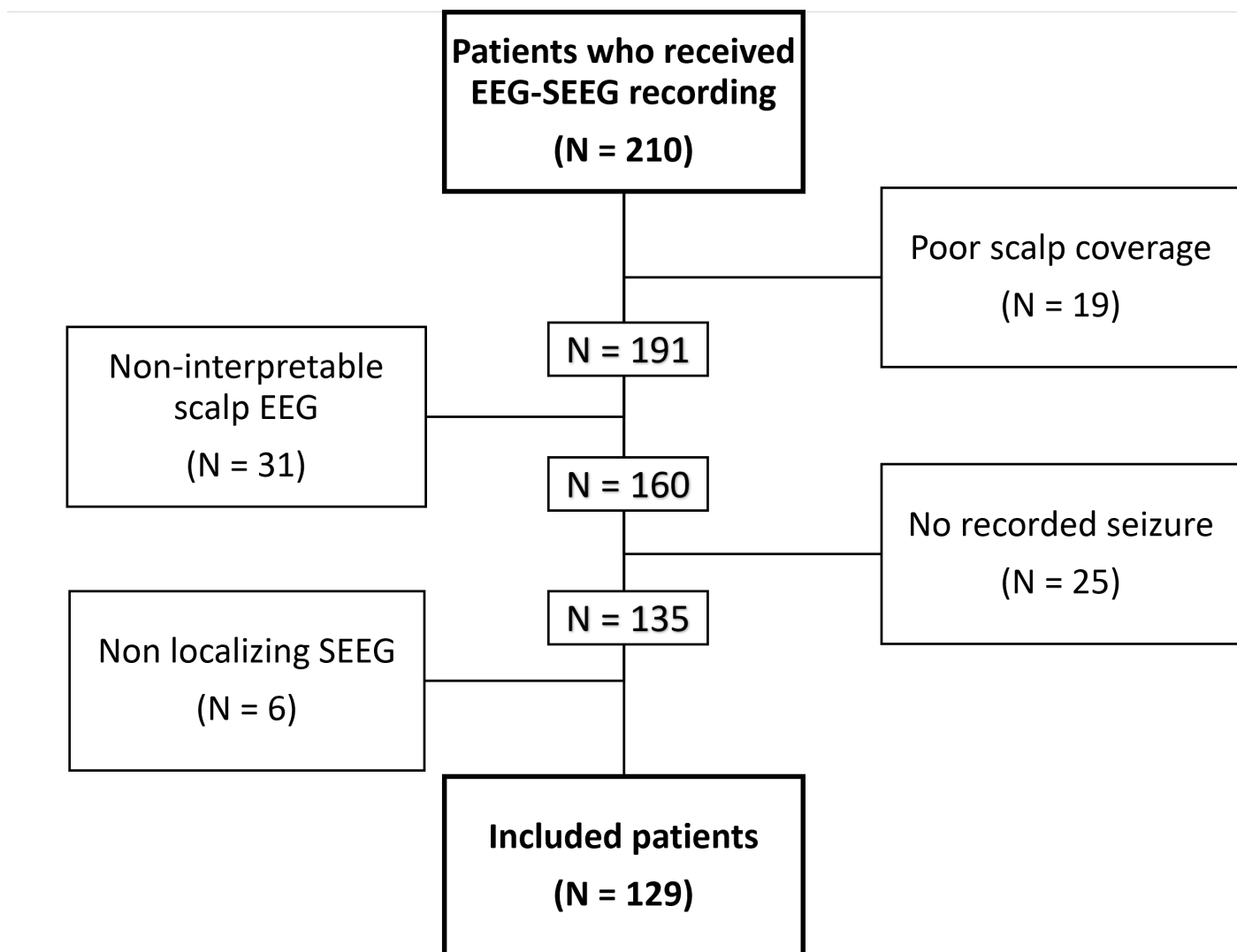


Figure 1: Flow-chart

Abbreviations: EEG = Electroencephalography; EZ = Epileptogenic zone; SEEG = Stereo Electroencephalography.

Cluster dendrogram: 1st scalp EEG abnormality

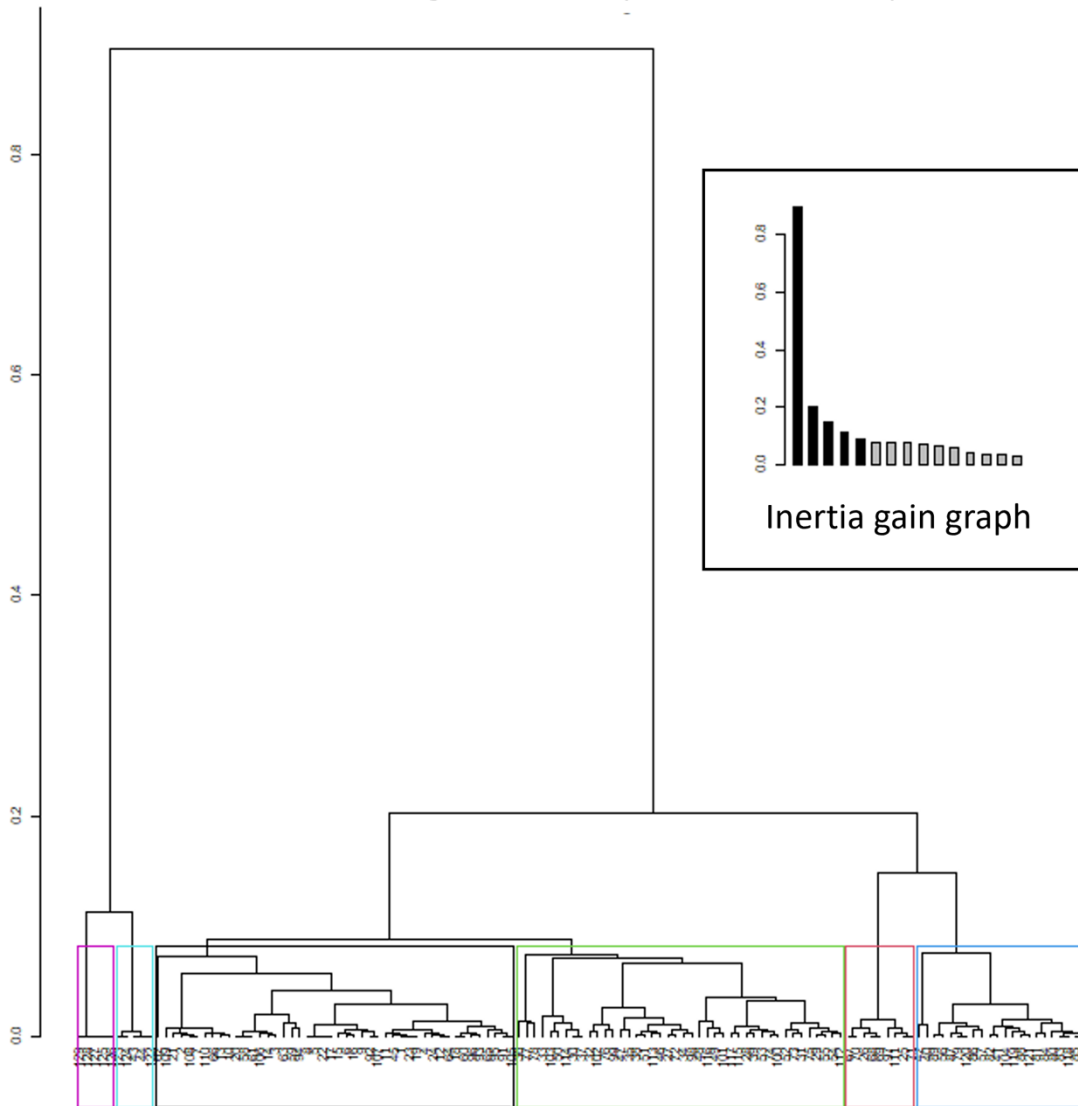


Figure 2: Hierarchical cluster analysis on the first scalp EEG abnormality

The hierarchical cluster analysis is performed by associating step by step, individuals (here the first abnormality of epileptic seizures in scalp EEG), then the groups already constituted, the closest in terms of modalities of their variables (by Euclidean distance) to finally form a dendrogram. The inertia gain graph is used to define the number of groups that will be formed. The first bar of the histogram represents the gain of inertia (the part of the variability between individuals) explained by going from one to 2 groups. The next bar represents the inertia gain by going from 2 to 3 groups etc. We have chosen to stop when the inertia gain reaches a plateau i.e., at 6 groups.

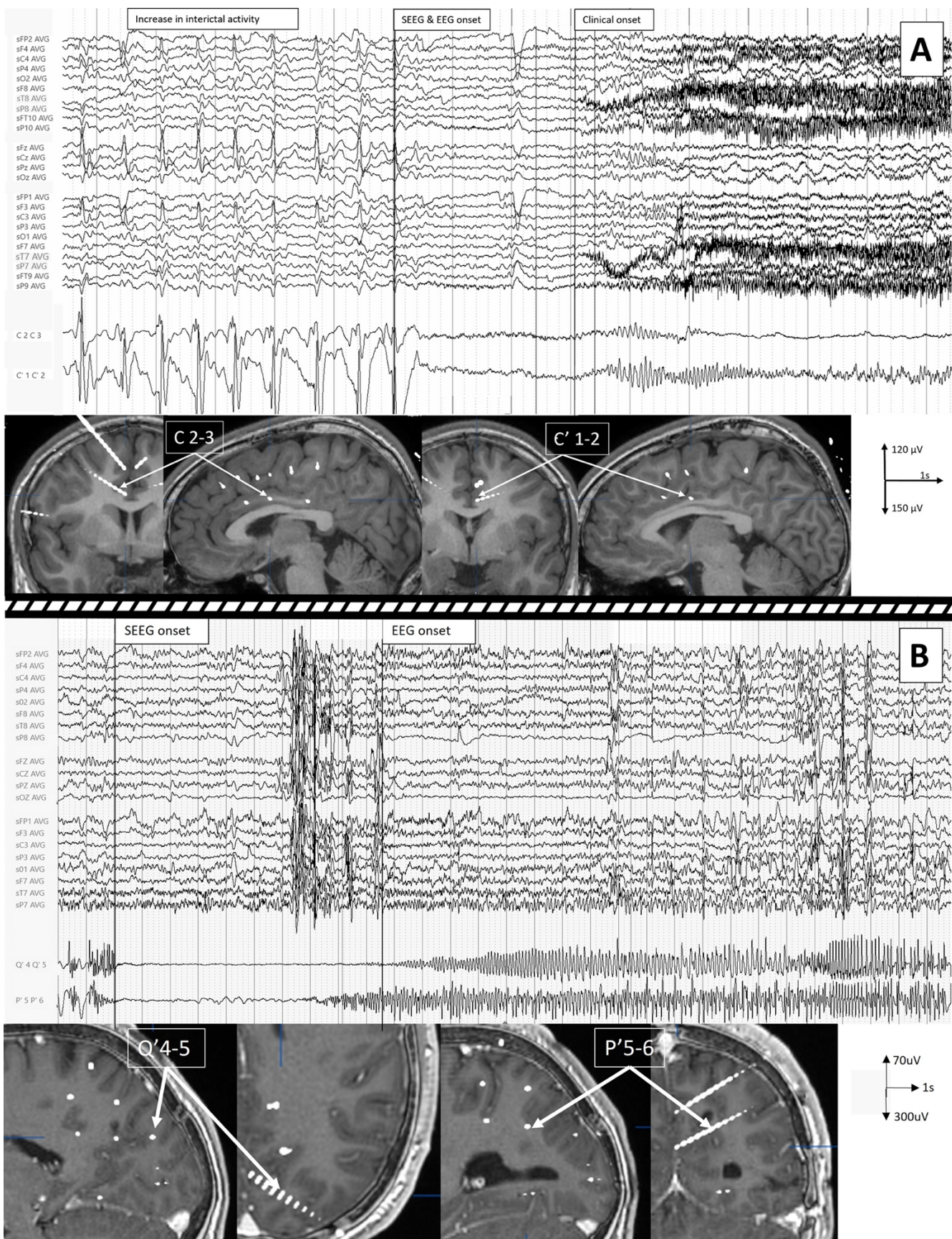


Figure 3: Simultaneous scalp EEG and SEEG recordings of a right premotor seizure (A) and a left parieto-occipital sulcus seizure (B).

A. The intra-cerebral recording shows a periodic inter-ictal activity (on the lower part of the recording). Then, the seizure starts on the right motor cingulate gyrus in C2-3 by a 40Hz low-voltage fast activity and spreads quickly contralaterally on the left motor cingulate gyrus (C'1-2). Inter-ictal activity is also visible on scalp EEG bilaterally on F4, C4, Fz, Cz, C3 (on the upper part of the recording). This inter-ictal activity stops at the onset of the seizure. Then emerges rhythmic activity at 20Hz on F4 and C4. Note that the clinical symptoms start 3 seconds after the seizure onset.

B. The intra-cerebral recording (on the lower part) shows a low-voltage fast activity beginning on the left parieto-occipital sulcus (internal contacts of P'). On the scalp EEG (on the upper part), the onset discharge appears 9 seconds after the SEEG onset, as rhythmic spikes discharge visible on P7, then P4, O2 et O1.

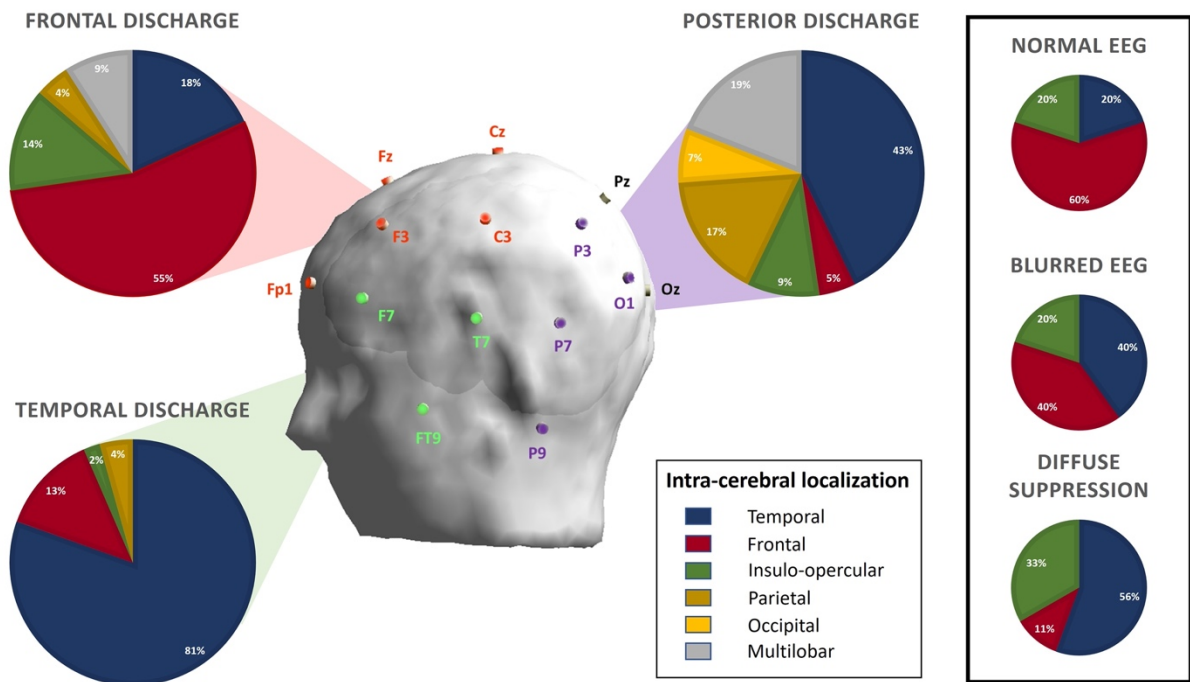


Figure 4: Correlations between scalp EEG discharge and intracerebral seizure onset localizations.

In the center, a representation of the localization of the electrodes according to the 10-20 system with a colorization of the electrodes according to their belonging to the different clusters.

In the periphery, a representation of the distribution of the intracerebral localizations of the onset of seizures by scalp cluster.

In the box on the right, the intracerebral localizations corresponding to normal EEG, blurred EEG, and diffuse suppression.